THE JOURNAL OF PHYSICAL CHEMISTRY B LETTERS

2005, *109,* 15182−15186
Published on Web 07/21/2005

Engineering a β-Sheet Protein toward the Folding Speed Limit

Houbi Nguyen,[†] Marcus Jäger,[§,||] Jeffery W. Kelly,*[,§] and Martin Gruebele*[,†,⊥]

Center for Biophysics and Computational Biology, University of Illinois, Urbana, Illinois 61801, Department of Chemistry and the Skaggs Institute for Chemical Biology, The Scripps Research Institute, 10550 North Torrey Pines Road MB12, La Jolla, California 92037, and Departments of Chemistry and Physics, University of Illinois, Urbana, Illinois 61801

Received: May 7, 2005; In Final Form: June 7, 2005

Recent experimental studies have shown that α-helical proteins can approach the folding "speed limit", where folding switches from an activated to a downhill process in free energy. β-sheet proteins are generally thought to fold more slowly than helix bundles. However, based on studies of hairpins, folding should still be able to approach the microsecond time scale. Here we demonstrate how the hPin1 WW domain, a triple-stranded β-sheet protein with a sharp thermodynamic melting transition, can be engineered toward the folding "speed limit" without a significant loss in thermal denaturation cooperativity.

Introduction

The energy landscape theory of protein folding makes an important prediction beyond earlier folding models: that proteins can fold without an activation barrier.[1] Folding downhill in free energy comes about when the decreasing folding enthalpy and entropy nearly cancel as the protein moves along the reaction coordinates toward the native state.[2]

Natural proteins have not evolved for rapid folding in particular.[3] However, proteins engineered for greater stability and faster folding kinetics have provided either direct evidence for downhill folding kinetics[4−6] or strong upper limits on the speed limit for folding.[7−11] The cases studied so far are helical or hairpin peptides and helical proteins. They reach the folding "speed limit" by folding within 0.5−2 μs,[5,7,12] in agreement with predictions.[13−15] The free energy surface of such proteins is not completely smooth. It retains residual free energy fluctuations that have been predicted,[15] computed,[16] and measured near $\delta^2G \approx 0.6\ k^2T^2$.[5,12] This free energy roughness lies below the minimum of 3 kT required to reliably apply transition state analysis. Thus, "downhill folders" fold nearly, but not quite, as fast as the contact formation time for a single loop (within 0.1 μs for protein-size loops).[17−19] Thermodynamic evidence for downhill folding, in the form of unusual baselines and of a probe-dependence of thermal denaturation transitions, has also been presented for small proteins and peptides,[20−22] whereas larger downhill folders shift to two state folding near the thermal denaturation midpoint.[6]

β-Sheet proteins are often thought of as slower folders. However, several experiments have shown that hairpin peptides can fold with observed relaxation time constants in the 0.7−3.5 μs range.[12,23] This time scale is quite comparable to those observed for helix bundles, opening up the question of whether β-sheet proteins can fold downhill or nearly so.

The human Pin1 WW domain is a very stable triple-stranded β-sheet protein with a sharp thermodynamic melting transition and a small but well-defined hydrophobic core (Figure 1).[24,25] We have studied the folding kinetics of this and related WW domains extensively.[26−28] The wild-type protein folds fairly fast (in 100 μs), but not near the speed limit. The 6-residue loop 1 of wild-type hPin1 WW domain is formed in the rate-limiting step. This loop has a one-residue insertion compared to most loops connecting the first and second β-strands in a typical WW domain, most likely because of functional evolutionary constraints.[29,30] A polarized transition state with rate-limiting loop formation was also observed for SH3 domains,[31,32] and the rate-limiting nature of longer loops has been investigated in a model system.[33]

For this study, we reengineered the wild-type protein to create variants with single-exponential kinetics and with a shortened or constrained loop 1. The folding rate was sped up from 10^4 s^{-1} for wild-type hPin1 WW domain to $\geq 10^5$ s^{-1} for the two fastest-folding variants. As fast and cooperatively folding β-sheet proteins, our variants should be of interest as targets for replica-exchange and single trajectory molecular dynamics simulations of refolding thermodynamics and kinetics.

Experimental Section

WW domains were prepared and purified as described previously,[27] except variant **4**, which was obtained commercially at >99% purity (Synpep Corp.). Our past work on Trp34-containing FBP WW domains revealed a slow kinetic phase contributing amplitude to the fluorescence lifetime signal.[28] We also recently observed such a phase during a structure−function-folding study on loop variants of Pin WW domain.[29] No such phase was observed for any point-mutants of Pin with the original 6-residue wild-type loop sequence (>100 mutants tested).[27]

* Corresponding authors.
[†] Center for Biophysics and Computational Biology, University of Illinois.
[§] The Scripps Research Institute.
[||] Present address: UCLA, Los Angeles, CA 90024.
[⊥] Departments of Chemistry and Physics, University of Illinois.

10.1021/jp052373y CCC: $30.25

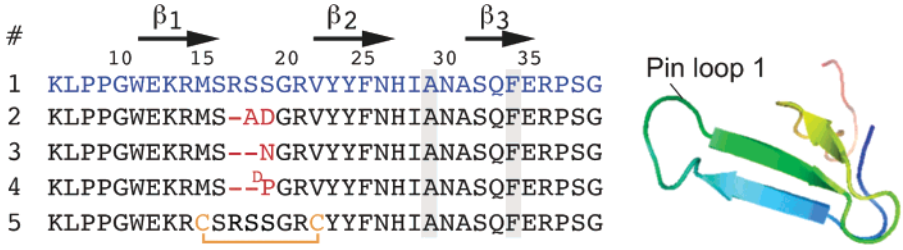

Figure 1. Mutants of hPin1 WW domain made for this study. The mutant with the unaltered loop 1 is shown in the top row, together with the conventional amino acid sequence numbering and identification of the β-strands. All proteins have the Thr29Ala and Trp34Phe mutations highlighted in gray. A structure of wild-type hPin1 WW domain is shown at the right for reference.

The slow phase can be eliminated by introducing a conservative Trp34Phe mutation into the Pin WW domain. All mutants studied here carry the Trp34Phe mutation. To bring the thermal folding/unfolding transitions fully within a temperature range accessible by temperature-jump experiments, we also destabilized the protein with the mutation Thr29Ala near loop 2. We previously showed that mutations of Pin WW domain near and in loop 2 have low Φ-values, so they have little effect on the rate-limiting step of folding.[27,34]

Sequence changes that speed up folding were made in the vicinity of loop 1 of the wild-type Pin WW domain, a region that limits the rate of native structure acquisition (Figure 1).[27] We made three variants by altering the sequence Arg17-Ser18-Ser19 of the wild-type **1** loop. Synthesis of a smaller 2 residue insert found in FBP WW domain produced **2**; a single-residue Asn insert capable of forming a type-I′ hairpin turn in the context of the flanking β-strand sequences afforded **3**; a ^{D}Pro insert capable of forming a type-II′ turn in the context of the neighboring residues yielded **4**. This is a particularly stable turn motif in the context of β-sheets. Further structural details motivating the choices of loops **1**, **2**, and **3** are given in our structure-function-folding study of a different series of WW domains.[29]

In addition, we created a double-cysteine variant **5** by engineering cysteine residues into positions 15 and 22 of the Pin sequence. These cysteines were then oxidized to form a disulfide bridge, reducing the conformational entropy of the hairpin formed by loop 1 and $\beta-$strands 1 and 2. Oxidation was achieved by first reducing the Cys residues by incubation with 10 mM dithiothreitol (DTT) for 6 h at ambient temperature, followed by gel-filtration to remove the reducing agent. Dialysis against 20 mM Tris, pH 8.0, 100 mM sodium chloride, 1 mM EDTA allowed formation of the intramolecular disulfide bond. Residual reduced protein was removed by adding a slurry of activated Thiol Sepharose 4B resin (Amersham Pharmacia), equilibrated in 20 mM Tris/100 mM sodium chloride at pH 8.0. After gentle shaking overnight at 4 °C, the supernatant was collected and concentrated, and contained only monomeric protein. Oxidized WW domain was isolated by gel filtration, dialyzed against 10 mM sodium phosphate and stored at 4 °C. All the WW domains used were monomeric and exhibited a maximum in the far-UV circular dichroism spectrum near 227 nm.

Thermodynamic data for the mutants were obtained as previously described[35] by monitoring the change in the circular dichroism spectrum at 227 nm as a function of temperature. Unfolding transitions of the reduced variant **5** were recorded in the presence of 20 mM DTT. Unfolding was reversible up to temperatures of 80 °C, above which hysteresis was evident in the melting curves. The Thr29Ala mutation ensured that all unfolding midpoints were well below 80 °C. We used a two-state model with a quadratic free energy dependence $\Delta G(T) = \Delta G_1(T - T_m) + \Delta G_1(T - T_m)^2$ to describe the equilibrium unfolding transitions, yielding melting temperatures T_m and free energy parameters ΔG_1.[35] Normalized unfolding transitions obtained at 10 and 100 μM were superimposable, indicating an absence of aggregation over the concentration range employed here (data not shown).

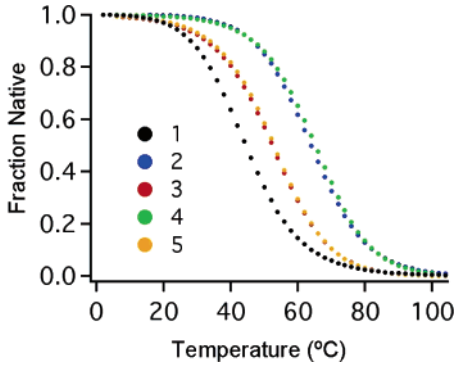

Figure 2. Thermal denaturation curves of hPin1 WW domain and its mutants show that all the variants have highly cooperative transitions, and all are more stable than the wild-type.

Relaxation kinetics were measured with a laser temperature-jump apparatus utilizing jumps between 6 and 15 °C.[36] Trp 11 was excited by a 292 nm laser pulse every 14 ns, and fluorescence emission decays were digitized at 500 ps intervals for 500 μs of data per measurement. The relaxation kinetics were obtained from the raw tryptophan fluorescence decays by using our previously reported χ-analysis.[37] The normalized curve of relaxation kinetics was fitted to a single exponential. Deviations from simple two-state behavior show up as nonexponential dynamics.[4] A two-state Kramers analysis,[38] with a conservative prefactor of 0.5 μs (see discussion) and a quadratic activation energy $\Delta G^{\ddagger}(T) = \Delta G_0^{\ddagger} + \Delta G_1^{\ddagger}(T - T_m) + \Delta G_2^{\ddagger}(T - T_m)^2$ was used to fit the temperature dependence of the observed relaxation rates. ΔG and $\Delta G^{\ddagger}$ were used to calculate separate folding and unfolding rates. However, for folding near the "speed limit", rates from a two-state analysis assuming an activation barrier should be considered nominal.

Results and Discussion

Protein Stability. All loop variants exhibit cooperative thermal melting transitions with well-defined pre- and post-transition baselines, as monitored by circular dichroism (Figure 2). Three stability categories emerge: the Pin WW Thr29Ala/Trp34Phe protein **1** is the least stable. Variants **3** and **5** (the short NG loop and the SS cross-link) are significantly ($\approx$10 °C increase in T_m) more stable than **1**. Variants **2** and **4** (the FBP loop insert and the short ^{D}Pro loop) are the most stable (by another $\approx$10 °C jump in T_m compared to **3** and **5**). Thermodynamic parameters (T_m, ΔG_1, and ΔG_2) from a two-state fit are listed in Table 1.

TABLE 1: Results from Nonlinear Least-Squares Fitting of the Thermal Denaturation Curves in Figure 2 and of the Kinetic Temperature Dependences in Figures 3 and 4[a]

no.	T_M (°C)	G_1 (kJ/mol/K)	G_2 (kJ/mol/K^2)	T_{max}, °C	τ_{obs} (μs)	$G_0^{\ddagger}$[b] (kJ/mol)*	$G_1^{\ddagger}$ (kJ/mol/K)*	$G_2^{\ddagger}$ (kJ/mol/K)*
1	45 (2)	0.3246 (26)	−0.0006 (21)	38 (2)	66 (4)	14.1 (1)	0.158 (7)	0.00339 (53)
2	64 (1)	0.3399 (35)	0.00060 (48)	65 (2)	5.0 (1.0)[c]	8.5 (1)	0.060 (6)	0.00422 (48)
3	52 (1)	0.3163 (55)	0.00167 (50)	51 (2)	19 (1)	11.7 (1)	0.0971 (94)	0.0050 (12)
4	65 (1)	0.3429 (69)	0.00169 (37)	68 (2)	4.5 (1.0)	8.1 (1)	0.0537 (66)	0.00518 (80)
5	53 (1)	0.3255 (43)	0.00179 (30)	54 (2)	6.5 (4)	15.5 (1)	0.0759 (74)	0.00692 (53)

[a] T_M is the melting temperature, T_{max} the temperature of maximum folding rate, and τ_{obs} the corresponding observed relaxation rate. [b] Activation free energies were calculated assuming a prefactor of 500 ns at 25 °C with an inverse bulk solvent viscosity dependence. [c] For **2**, the kinetic fit is the best single-exponential fit, with a small deviation below 3 μs. Estimated errors are given in parentheses.

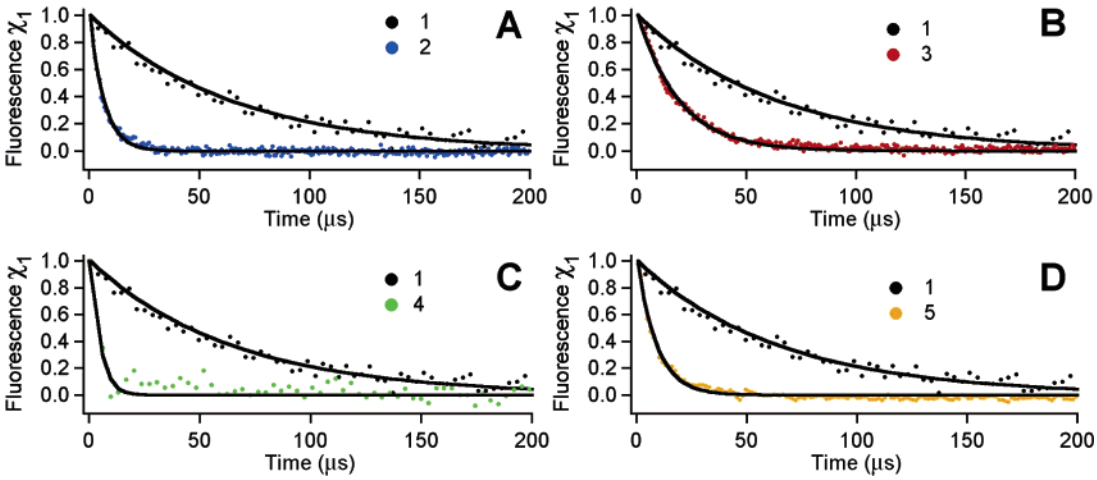

Figure 3. Kinetic relaxation traces near the temperature of maximal folding rate. The black curves are single-exponential fits to the data. (A) Comparison of variants 1 and 2; (B) Comparison of variants 1 and 3; (C) Comparison of variants 1 and 4; (D) Comparison of variants 1 and 5.

The reduced Met15Cys/Val22Cys variant is less stable than **1** (data not shown), consistent with previous alanine substitutions at these positions.[27] Oxidative formation of a cross-strand disulfide bond greatly stabilizes the variant (Figure 2, Table 1). The extent of stabilization (−3.4 kJ mol^{-1} at 54 °C) agrees well with loop entropy estimates of $-1.5RT \ln(L_{WT}/L_{SS}) \approx -4.5$ kJ mol^{-1}, where $L_{WT} = 6$ and $L_{SS} = 2$ are the effective loop lengths of **1** and **5**.[39,40] The higher stability of the oxidized domain therefore appears largely due to an entropic destabilization of the denatured state. The disulfide variant makes loop 1 registry during folding unnecessary, removing the obstacle of forming a six residue loop.

The short NG loop variant **3** is not nearly as stable as the longer variant **2**. This result is unexpected when only loop-occurrence statistics are considered because (2:2) type-I′ turns are the most abundant turn types found in short β-hairpin substructures.[40−42] Other factors, such as loop stiffness, or geometrical constraints on the WW scaffold from hydrophobic core constraints and β-sheet twisting (Figure 1), must be taken into account.

Folding Kinetics. All variants can be fitted reasonably accurately by single-exponential relaxation profiles after T-jumps between 6 and 15 °C. Representative traces, obtained at the temperature of fastest refolding are shown in Figure 3.

Variants **2**, **3**, **4**, and **5** all fold much faster than the hPin1 pseudo wild-type reference protein **1**. The same trend is also observed under iso-free energy conditions (at $T = T_M$ where $\Delta G = 0$, see Table 1). The observed relaxation rate of variant **5** is $k_{obs} \approx 1.1\ \mu s^{-1}$ in Figure 3. A very small deviation from single-exponential kinetics was observed for variant **2**. Similar deviations have been previously reported as signatures of downhill folding.[4] However, the signal-to-noise ratio of kinetic traces obtained for variants **2** and **5** reliably determines only one phase.

The equilibrium data and two-state assumption $k_{obs} = k_f + k_u$ were used to obtain the activation energy parameters shown in Table 1. Arrhenius plots of the resulting refolding and unfolding rates are depicted in Figure 4. The unfolding plots are curved but with negative slope. All mutants exhibit non-Arrhenius behavior with a decrease in folding rate at higher temperatures. Maximal refolding rates of 1×10^4 s^{-1} (**1**, 38 °C), 3×10^4 s^{-1} (**3**, 51 °C), 7×10^4 s^{-1} (**5**, 54 °C), 1×10^5 s^{-1} (**2**, 65 °C), and 1.1×10^5 s^{-1} (**4**, 68 °C) are obtained. Except for variant **1**, the temperature T_{max} at which the folding rate is maximized lies very close to the thermal denaturation midpoint T_M (Table 1). As T_M increases, ln k_f increases nearly linearly for the fast mutants **2** through **5** (dotted line in Figure 4A). Such a strong thermodynamics-kinetics correlation is expected either for a very late transition state, or in the absence of a significant folding barrier.[43]

Loop variants **2** and **4** fold significantly faster than the FBP28 WW domain, the fastest folding β-sheet protein known to date.[28] The effect of loop redesign manifests itself predominantly in faster refolding, while the unfolding rates are little affected (as can be calculated from the data in Table 1). This is expected if both the ground state and transition state are significantly stabilized by the loop 1 modifications, and if formation of the hydrophobic core as well as formation of the loop 2 region are intrinsically fast and masked by the rate limiting formation of loop 1 in wild-type hPin1. Thus our current results support our earlier Φ-value analysis, which indicated that loop 2 and the core are formed at lower free energy than loop 1.[27] It would thus be interesting to repeat our previous Φ-analysis in the context of the redesigned loop 1 region to see whether the rate-limiting step indeed switches from loop 1 to loop 2, as shown previously for the Protein L/Protein G pair by Baker and co-workers.[44]

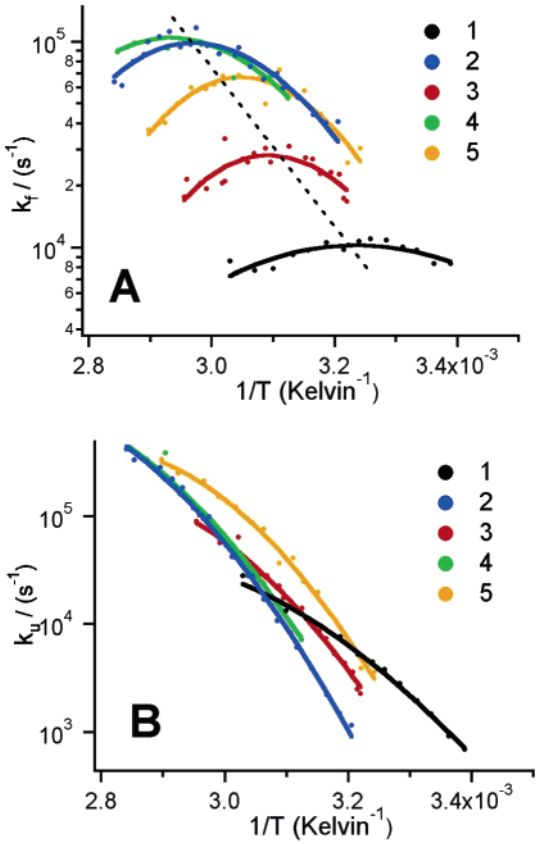

Figure 4. (A) Refolding rates computed using the two-state folding assumption, showing non-Arrhenius curvature and a temperature of maximal folding rate. The colored fitted curves use the activation parameters in Table 1. The dashed line is a visual aid to show the nearly linear correlation between $\ln[k_f]$ and $1/T_{max}$, where the folding rate maximum occurs. (B) Corresponding unfolding rates.

Comparison with the Folding "Speed Limit". The "speed limit" for folding has been estimated to occur on a time scale of 1 μs.[13,14] It was measured to be 1−2 μs for mutants of a 5-helix bundle by observing a phase due to downhill diffusion, as well as probe-dependent kinetics.[4,6] Smaller proteins have set upper limits as low as 0.5 μs,[2,7,9] depending on the size of the protein. For β-sheet proteins, there are currently no direct measurements, but the trpzip2 β-hairpin peptide sets an upper limit of 0.7 μs on hairpin formation times,[12,45] and the first β-hairpin to have its relaxation rate measured equilibrated in 3.5 μs.[23] Using the lower 0.5 μs value from these results as a conservative estimate of the prefactor, we obtain a barrier of 3.5 kT for **2**, very near the downhill folding limit. Accordingly, variants **2** and **5** lie close to the upper limiting rate on a plot of ln k_f vs absolute contact order.[5] This is to be compared with a barrier of 5.5 kT estimated for **1**, which can be described accurately by an activated Kramers model.

Fast Folding and Cooperativity. Downhill folding within a single well is associated with a loss of cooperativity.[20] Yet like the five-helix bundle λ_{6-85},[6] hPin1 WW variants **2** and **4** show no loss of cooperativity (all mid-denaturation slopes are the same in Figure 2). This observation has been explained and modeled quantitatively by a downhill to two-state transition induced by raising the temperature:[6] as the free energy of the native state increases upon heating, so does the free energy of the transition region, creating a barrier. This downhill to two-state transition was first postulated as the "type 0" to "type 1" transition in energy landscape theory.[1] It implies that a cooperative melting transition cannot be used to infer two-state folding at lower temperatures where the native state is more stable.

Conclusions

The triple-stranded β-sheet protein hPin1 can be reengineered in loop 1 to increase the folding rate by over a factor of 10, to greater than 0.1 μs^{-1}. The estimated residual folding barrier is $\leq$3.5 kT. It remains to be seen whether hPin1 mutants could also display direct diagnostics of downhill folding, such as probe-dependent kinetics,[6,12] a fast "molecular" phase preceding the activated kinetics,[4] or different viscosity dependences for the molecular and activated phases of the kinetics.[5] Furthermore, although it would preclude characterization over the full temperature range done here, removal of the Thr29Ala mutation would further speed up the kinetics. In addition, the −ADG (variant **2**) and - -NG (variants **3** and **4**) loop motifs are excellent starting points for further variations of the type −XDG and - -XG to enhance folding rates. The size of the hPin1 WW domain coupled with its very fast folding makes it an attractive target for state-of-the-art replica exchange and single trajectory molecular dynamics simulation studies.

Acknowledgment. H.N. and M.J. contributed equally to this work. M.J. would like to acknowledge the La Jolla Interfaces in Science program for fellowship support while this work was carried out. M.G. and H.N. were supported by NSF Grant MCB 0316925. J.K. and M.J. were supported by NIH Grant GM 051105, the Skaggs Institute of Chemical Biology, and the Lita Annenberg Hazen Foundation.

References and Notes

(1) Bryngelson, J. D.; Onuchic, J. N.; Socci, N. D.; Wolynes, P. G. *Proteins: Struct., Funct., Genet.* **1995**, *21*, 167.
(2) Kubelka, J.; Hofrichter, J.; Eaton, W. A. *Curr. Opinion Struct. Biol.* **2004**, *14*, 76.
(3) Kim, D. E.; Gu, H.; Baker, D. *Proc. Natl. Acad. Sci. U.S.A.* **1998**, *95*, 4982.
(4) Yang, W. Y.; Gruebele, M. *Nature* **2003**, *423*, 193.
(5) Yang, W.; Gruebele, M. *Biophys. J.* **2004**, *87*, 596.
(6) Ma, H.; Gruebele, M. *Proc. Natl. Acad. Sci. U.S.A.* **2005**, *102*, 2283.
(7) Zhu, Y.; Alonso, D. O. V.; Maki, K.; Huang, C.-Y.; Lahr, S. J.; Daggett, V.; Roder, H.; DeGrado, W. F.; Gai, F. *Proc. Natl. Acad. Sci.* **2003**, *100*, 15486.
(8) Arora, P.; Oas, T. G.; Myers, J. K. *Protein Sci.* **2004**, *13*, 847.
(9) Qiu, L. L.; Pabit, S. A.; Roitberg, A. E.; Hagen, S. J. *J. Am. Chem. Soc.* **2002**, *124*, 12952.
(10) Kubelka, J.; Eaton, W. A.; Hofrichter, J. *J. Mol. Biol.* **2003**, *329*, 625.
(11) Faraone-Mennella, J.; Gray, H. B.; Winkler, J. R. *Proc. Natl. Acad. Sci. U.S.A.* **2005**, *102*, 6315.
(12) Yang, W. Y.; Gruebele, M. *J. Am. Chem. Soc.* **2004**, *126*, 7758.
(13) Camacho, C. J.; Thirumalai, D. *J. Physique I* **1995**, *5*.
(14) Hagen, S. J.; Hofrichter, J.; Szabo, A.; Eaton, W. A. *Proc. Natl. Acad. Sci. U.S.A.* **1996**, *93*, 11615.
(15) Portman, J. J.; Takada, S.; Wolynes, P. G. *J. Chem. Phys.* **2001**, *114*, 5069.
(16) Shea, J.; Brooks, C. L. *Annu. Rev. Phys. Chem.* **2001**, *52*, 499.
(17) Eaton, W. A.; Muñoz, V.; Thompson, P. A.; Henry, E. R.; Hofrichter, J. *Acc. Chem. Res.* **1998**, *31*, 745.
(18) Bieri, O.; Wirz, J.; Hellrung, B.; Schutkowski, M.; Drewello, M.; Kiefhaber, T. *Proc. Natl. Acad. Sci. U.S.A.* **1999**, *96*, 9597.
(19) Chang, I. J.; Lee, J. C.; Winkler, J. R.; Gray, H. B. *Proc. Natl. Acad. Sci. U.S.A.* **2003**, *100*, 3838.
(20) Muñoz, V. *Int. J. Quantum Chem.* **2002**, *90*, 1522.
(21) Garcia-Mira, M. M.; Sadqi, M.; Fischer, N.; Sanchez-Ruiz, J. M.; Muñoz, V. *Science* **2002**, *298*, 2191.
(22) Yang, W. Y.; Pitera, J.; Swopes, W.; Gruebele, M. *J. Mol. Biol.* **2004**, *336*, 241.
(23) Muñoz, V.; Thompson, P. A.; Hofrichter, J.; Eaton, W. A. *Nature* **1997**, *390*, 196.
(24) Koepf, E. K.; Petrassi, H. M.; Sudol, M.; Kelly, J. W. *Protein Sci.* **1999**, *8*, 841.
(25) Kowalski, J. A.; Liu, K.; Kelly, J. W. *Biopolymers* **2002**, *63*, 111.
(26) Crane, J. C.; Koepf, E. K.; Kelly, J. W.; Gruebele, M. *J. Mol. Biol.* **2000**, *298*, 283.
(27) Jäger, M.; Nguyen, H.; Crane, J.; Kelly, J.; Gruebele, M. *J. Mol. Biol.* **2001**, *311*, 373.

(28) Nguyen, H.; Jäger, M.; Gruebele, M.; Kelly, J. *Proc. Natl. Acad. Sci. U.S.A.* **2003**, *100*, 3948.
(29) Jäger, M.; Nguyen, H.; Dendle, G.; Gruebele, M.; Kelly, J. *Proc. Natl. Acad. Sci. U.S.A.* **2005**, submitted for publication.
(30) Verdecia, M. A.; Bowman, M. E.; KP, K. P. L.; Hunter, T.; Noel, J. P. *Nat. Struct. Biol.* **2000**, *7*, 639.
(31) Grantcharova, V. P.; Riddle, D. S.; Santiago, J. V.; Baker, D. *Nat. Struct. Biol.* **1998**, *5*, 714.
(32) Martinez, J. C.; Pisabarro, M. T.; Serrano, L. *Nat. Struct. Biol.* **1998**, *5*, 721.
(33) Dyer, R. B.; Maness, S. J.; Peterson, E. S.; Franzen, S.; Fesinmeyer, R. M.; Andersen, N. H. *Biochemistry* **2004**, *43*.
(34) Deechongkit, S.; Nguyen, H.; Powers, E. T.; Dawson, P. E.; Gruebele, M.; Kelly, J. W. *Nature* **2004**, *430*, 101.
(35) Jäger, M.; Nguyen, H.; Kelly, J.; Gruebele, M. *Proc. Natl. Acad. Sci. U.S.A.* **2004**, submitted for publication.
(36) Ballew, R. M.; Sabelko, J.; Reiner, C.; Gruebele, M. *Rev. Sci. Instrum.* **1996**, *67*, 3694.
(37) Ervin, J.; Sabelko, J.; Gruebele, M. *J. Photochem. Photobiol.* **2000**, *B54*, 1.
(38) Kramers, H. A. *Physica* **1940**, *7*, 284.
(39) Jacobsen, H.; Stockmeyer, W. H. *J. Chem. Phys.* **1950**, *18*, 1600.
(40) Grantcharova, V. P.; Riddle, D. S.; Baker, D. *Proc. Natl. Acad. Sci. U.S.A.* **2000**, *97*, 7084.
(41) Sibanda, B. L.; Thornton, J. M. *Methods Enzymol.* **1991**, *202*, 59.
(42) Gunasekaran, K.; Ramakrishnan, C.; Balaram, P. *Protein Eng.* **1997**, *10*, 1131.
(43) Larios, E.; Pitera, J.; Swope, W.; Gruebele, M. *Chem. Phys.* **2005**, submitted for publication.
(44) Nauli, S.; Kuhlman, B.; Baker, D. *Nat. Struct. Biol.* **2001**, *8*, 602.
(45) Snow, C. D.; Qiu, L. L.; Du, D. G.; Gai, F.; Hagen, S. J.; Pande, V. S. *Proc. Natl. Acad. Sci. U.S.A.* **2004**, *101*, 4077.